Reprinted from the preprint volume of SEVENTH CONFERENCE ON SATELLITE METEOROLOGY AND OCEANOGRAPHY. June 6–10, 1994. Monterey, CA.
Published by the American Meteorological Society, Boston, MA.

P3.5

SOME REGIONAL CHARACTERISTICS OF OCEANIC RAINFALL AND THEIR IMPLICATIONS FOR SATELLITE RAINFALL RETRIEVALS

Grant W. Petty*

Purdue University
West Lafayette, Indiana

1 INTRODUCTION

In the ongoing quest for satellite-derived climatologies of precipitation — whether in the context of the Tropical Rainfall Measuring Mission (TRMM), the Global Precipitation Climatology Project (GPCP, or some other initiative — it has been tacitly assumed that, with sufficient effort and care, algorithms *can* in principle be developed that give approximately the right answer (say, to within 10% over 5° boxes) everywhere over the global oceans, or at least over large, well-defined climate zones. This in turn requires either (1) that the satellite signature of precipitation be essentially the same everywhere within the target region (e.g., the tropics) or else (2) that algorithms can be made intelligent enough to recognize (or at least know about) and account for regional variations in precipitation signatures.

While progress in the latter endeavor may yet be forthcoming, it will be difficult for at least the immediate future for even the most elaborate, physically grounded algorithms to overcome the constraints imposed by less-than-ideal sampling, spatial resolution, and spectral diversity. In the meantime, much current rain rate retrieval work continues to focus on the calibration of empirical algorithms over the very limited regions for which surface validation data is available, followed by their utilization for the production of a variety of global rainfall climatologies intended for use by the broader scientific community.

The purpose of this paper is to present data suggestive of the potential hazards of extrapolating satellite algorithm performance from the limited calibrated regions to the vast uncalibrated regions of the global oceans.

* *Corresponding Author Address:* Grant W. Petty, Earth and Atmospheric Sciences Dept., West Lafayette, IN, 47907-1397

2 POTENTIAL ERROR SOURCES IN GLOBAL RAINFALL ESTIMATES

All satellite rain rate retrieval techniques — whether microwave or infrared — are sensitive to deviations in certain properties of the rainfall from those encountered or assumed during the algorithm's calibration. Infrared algorithms generally assume a reasonably constant relationship between cloud top temperature and surface rain rate; it is well known that this relationship often fails for stratiform and/or shallow warm-cloud or orographic rain. Microwave algorithms of the "emission" variety are subject to the so-called footprint-filling bias, which depends on the degree of spatial inhomogeneity of the rainfall. Often, a single global footprint-filling bias correction is assumed, based perhaps on empirical studies of rainfall statistics in a specific data set, such as that from GATE. Scattering-based algorithms, on the other hand, must assume a constant relationship between the observed scattering of radiation by ice particles aloft and surface rainfall, notwithstanding the fact that this relationship may be strongly sensitive to the microphysical characteristics of the rain cloud in question.

3 VARIATIONS IN OCEANIC PRECIPITATION BASED ON SSM/I DATA

We have processed one year's worth of global oceanic SSM/I data in an effort to uncover systematic regional variations in the apparent physical character of precipitation. We base our analysis on the normalized 37 GHz polarization P_{37} and an 85.5 GHz scattering index S_{85} — see Petty and Stettner (1994; this volume) and references therein. Here it is sufficient to note that $P_{37} < 0.5$ is considered, based on both theoretical and empirical evidence, to be an unambiguous indication of liquid precipitation filling a significant portion of the 37 GHz field of view. By contrast, the scattering index S_{85} is largely insensi-

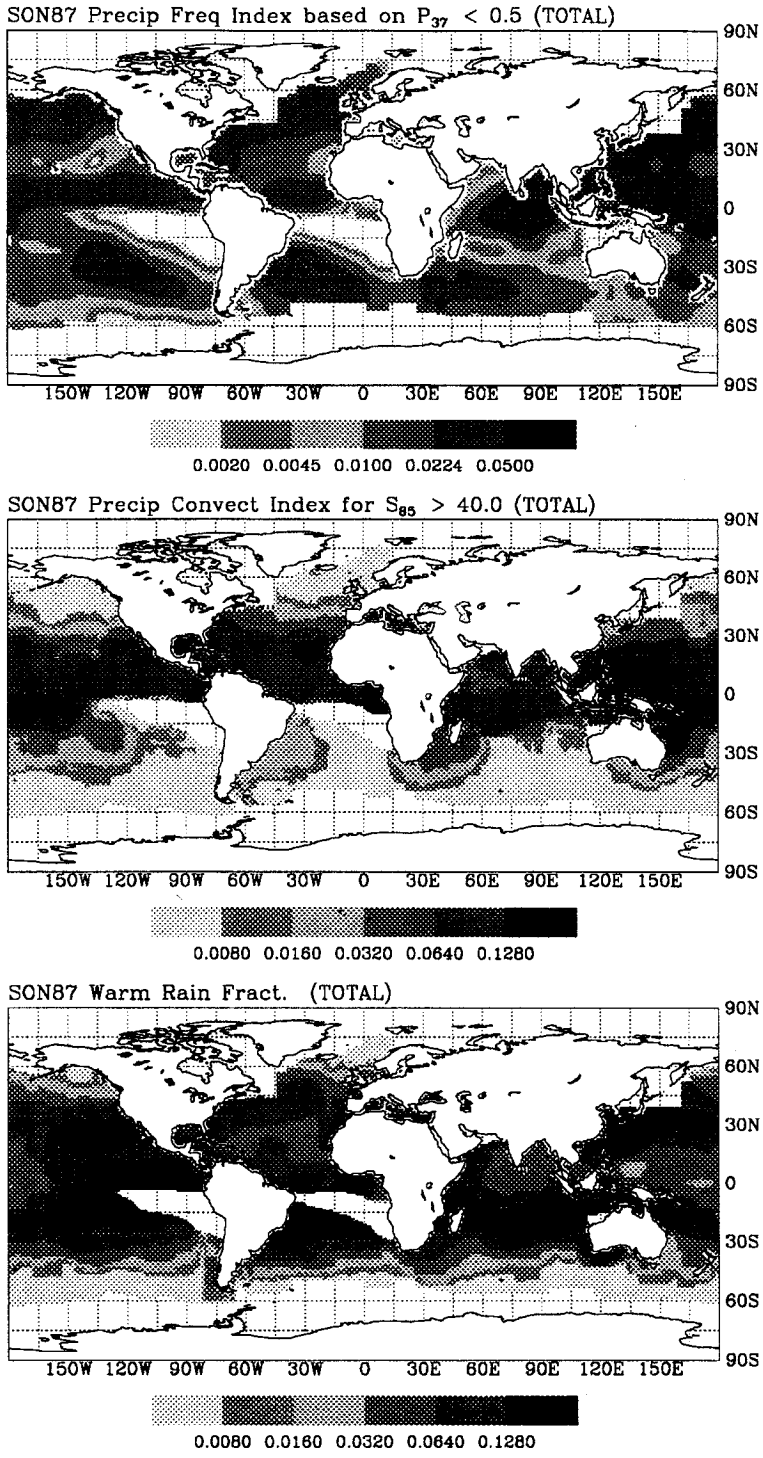

Fig. 1: Rainfall frequencies and characteristics inferred from SSM/I brightness temperatures for SON 1987. Top: Raw precipitation frequency index, based on $P_{37} < 0.5$. Middle: Fraction of precipitating pixels exhibiting strong 85 GHz scattering ($S_{85} > 40$ K) and thus likely to be associated with deep convection. Bottom: Fraction of precipitating pixels exhibiting no 85 GHz scattering ($S_{85} < 0$ K) and thus likely to be associated with warm cloud rainfall.

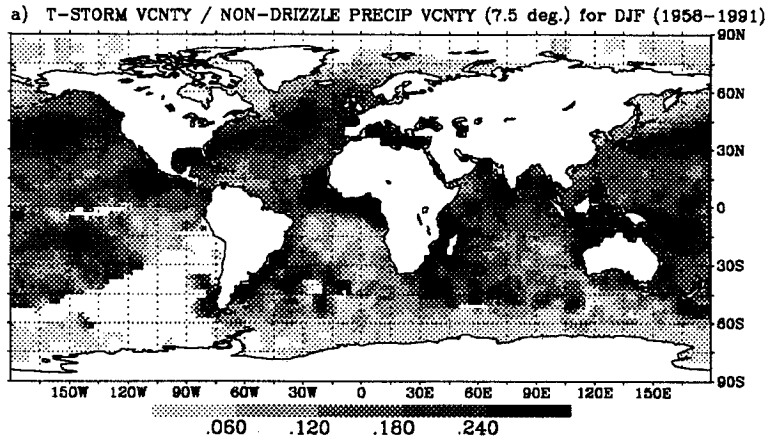

Fig. 2: COADS present weather reports indicating thunderstorm activity, as fraction of all non-drizzle intensity precipitation reports.

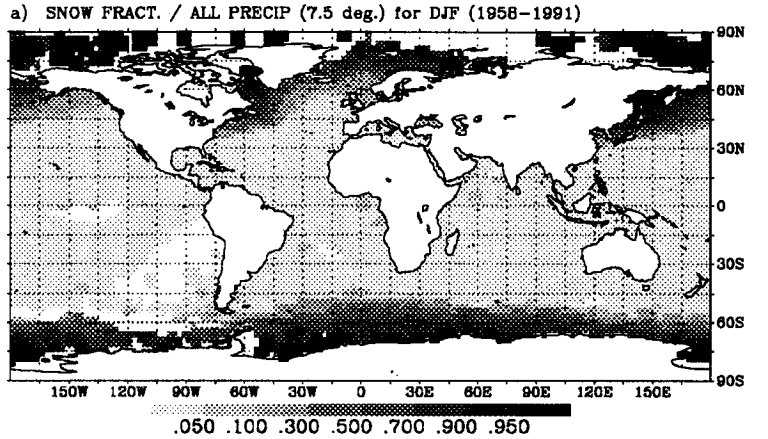

Fig. 3: COADS present weather reports indicating snowfall, as fraction of all precipitation reports.

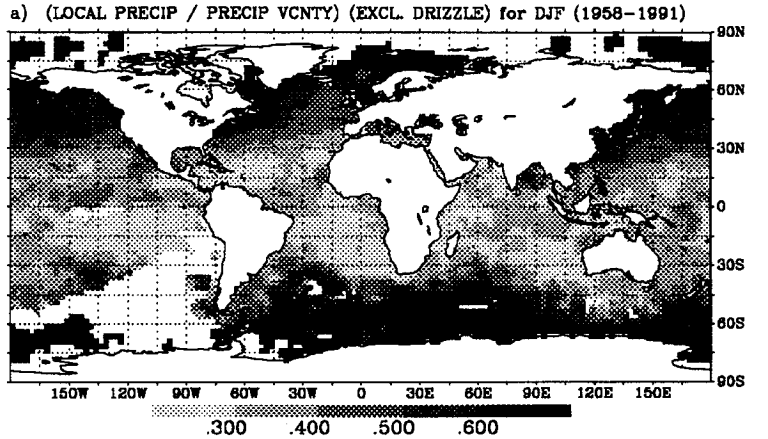

Fig. 4: COADS present weather reports indicating precipitation at the ship and at the time of the observation, as fraction of all precipitation reports, including precipitation observed near but not at the station and precipitation at the station during the previous hour but not at the time of observation.

tive to the liquid water component of the rain cloud and responds primarily to precipitation size ice particles aloft, such as graupel and snow. Thus, values of $S_{85} > 40$ K are taken to be strongly suggestive of pronounced cold-cloud convective process capable of supporting the production of large ice particles.

Counts of SSM/I pixels with normalized 37 GHz polarization $P_{37} < 0.5$ were tallied over 2.5° grid boxes for three month periods. This count, expressed as a fraction of the total sample and smoothed with a 15° window, is depicted in Fig. 1 (top) for SON 1987. Second, for those pixels satisfying the above criterion, the associated values of S_{85} were analyzed. Figure 1 (middle) depicts the fraction of raining pixels for which $S_{85} > 40$ K, indicating the apparent frequency with which the liquid precipitation observed by way of P_{37} is associated with strong convection.

Similarly, raining pixels were tallied for which $S_{85} < 0$ K. Since this value implies an effective emitting temperature greater than 273 K, Fig. 1 (bottom) may be interpreted as a map of the frequency of apparent warm cloud precipitation, expressed as a fraction of the total precipitation frequency.

While space does not permit a detailed discussion, it is apparent that the relative predominance of cold cloud convection and of apparent warm cloud rainfall varies sharply from region to region, even within the tropics. Interestingly, the two maps are not mirror images of one another. To the extent that satellite algorithms assume a certain component of convective cloudiness or are insensitive to warm-cloud precipitation, it would appear that the potential for regional biases is very high.

4 VARIATIONS IN OCEANIC PRECIPITATION BASED ON COADS DATA

A different perspective on the variability of oceanic rainfall is obtained through the analysis of a 34 year record (1958-1991) of shipboard present weather reports from the Comprehensive Ocean-Atmosphere Data Set (COADS). Here, the occurrence of various classes of precipitation was tallied over 2.5° grid boxes and the frequencies of these classes compared with one another.

Figure 2 shows the fraction of precipitation reports (excluding drizzle intensity) clearly identified with some form of thunderstorm activity during the 3 months of December-January-February. There is up to a factor of 4 variability in the relative predominance of thunderstorm activity, even along the ITCZ. Interestingly, the most active regions for thunderstorms (conditioned on the occurrence of precipitation) are confined to the vicinity of the land masses. Moreover, virtually all of the important ground truth sites for satellite oceanic rainfall estimation are located within these very active regions. To the extent that the satellite-observed signature of precipitation is influenced by microphysical processes connected to thunderstorm development, these results again suggest a potential for regional biases.

For microwave emission algorithms, it is generally assumed that significant quantities of rain water must be present in order for the precipitation to be detected, owing to the relative transparency of ice. Fig. 3 delineates the climatological frequency of snow, conditioned on the occurrence of precipitation.

By comparing the frequency of *all* precipitation reports — including those of precipitation within the previous hour and/or visible at a distance from the station — with that of precipitation occurring at the station at the time of the observation, it is possible to obtain a qualitative map of the relative homogeneity of precipitation in both space and time (Fig. 4). The ratio of instantaneous local precipitation to all precipitation is quite high in the high latitudes, implying a predominance of steady stratiform precipitation. In the tropics and subtropics, by contrast, rainfall is evidently quite showery, as indicated by ratios falling below 30%. Although not shown here, the COADS data reveal that precipitation is not at all uncommon in the subtropical high zones west of South America and Africa, despite the common failure of satellite microwave algorithms to detect it at all over month-long sample periods. The data in Fig. 4 suggest that precipitation in these regions is very transient and showery and therefore impossible to detect with even the 15 km resolution of the SSM/I's 85 GHz channels.

Acknowledgments

This work was supported by NASA Grant NAGW-2984. COADS data were provide by the Scientific Computing Division/Data Support Services at the National Center for Atmospheric Research.

REFERENCES

Petty, G.W., and D.R. Stettner, 1994: A new inversion-based algorithm for retrieval of overwater rain rate from SSM/I multichannel imagery. *7th Conference on Satellite Meteorology and Oceanography*, Monterey, California, 6–10 June. (this volume).